

LA-UR -94-100

Los Alamos National Laboratory is operated by the University of California under contract with the United States Department of Energy. File number LA-UR-94-1005 ENG-36

TITLE: Reflected-Shock Initiation of Explosives

AUG 05

AUTHOR(S) Eric N. Form, LANL, M-8
Lawrence M. Hull, LANL, M-8

SUBMITTED TO Tenth International Detonation Symposium

DISCLAIMER

This report was prepared as an account of work sponsored by an agency of the United States Government. Neither the United States Government nor any agency thereof, nor any of their employees, makes any warranty, express or implied, or assumes any legal liability or responsibility for the accuracy, completeness, or usefulness of any information, apparatus, product, or process disclosed, or represents that its use would not infringe privately owned rights. Reference herein to any specific commercial product, process, or service by trade name, trademark, manufacturer, or otherwise does not necessarily constitute or imply its endorsement, recommendation, or favoring by the United States Government or any agency thereof. The views and opinions of authors expressed herein do not necessarily state or reflect those of the United States Government or any agency thereof.

Reproduction of this work or the disclosure of its contents to persons other than the contractor without the written consent of the contractor is prohibited by law. The contractor retains a nonexclusive, irrevocable license to use this work for Government purposes.

The United States Government expressly disclaims that the disclosure, transfer, or release of this document does not constitute an assignment of copyright.

John M. Form

Los Alamos Los Alamos National Laboratory
Los Alamos, New Mexico 87545

REFLECTED-SHOCK INITIATION OF EXPLOSIVES

E. N. Fermi and L. M. Hull

Explosives Technology and Applications Division
Los Alamos National Laboratory
Los Alamos, New Mexico 87545

In a study of initiations caused by reflected shock front a high-impedance boundary attempts to establish sufficient conditions for initiation are described. Shock polar analysis is used to discover the ranges of various flow regimes, general shock structures and pressure estimates of states behind the reflected wave. Using this knowledge, wave structure growth rates from hydrocode simulations are estimated and standard-shock initiation criteria are used; experiments are designed in which the initiation from a reflected-shock wave structure appears likely. Two experiments are described in which a reflected shock wave from a titanium surface initiated PBX 9502. The experimental evidence is in good agreement with the assumptions and results of the analysis.

INTRODUCTION

Shock initiation of explosives has been studied extensively and has resulted in useful models that describe the rate to detonation, given the initial shock pressure. The experiments leading to these models were designed to eliminate boundary effects. The work presented here studies the influence of high-impedance boundaries on shock initiation of explosives. When boundaries are included in the problem, more analysis is required to determine the effect of wave reflections from the boundaries. Our approach to this problem was to examine the shock structure of the nonreactive reflected wave problem using shock polar analysis and hydrocode simulations. We then looked for the shock structures that appear likely to initiate the explosive, considering the known explosive properties.

To obtain the shock structure, we studied the simple geometrical configuration of the reflection of a nonreactive, planar shock traveling in the explosive impacting a flat high-impedance metal plate like titanium. In this case, classical shock polar theory applies. This simple analysis determines the pressure behind the reflected wave as a function of the interaction angle and incident shock pressure. If the wave reflection is regular, the incident wave and the reflected wave are attached to the wall. If it is irregular, a more complicated shock structure must exist between the incident and reflected shock and the wall in order to satisfy boundary conditions. Shock polar analysis is only a local analysis, and it has limitations because the flow configurations are assumed in order to do the analysis. Our hydrocode calculations of the wave reflection problem were made to validate the shock polar analysis and to obtain growth-rate information of the irregular reflection.

To find a case in which a reflected shock is likely to initiate an explosive, we expected the following conditions must be met: (1) the incident shock must not decelerate the explosive,¹ (2) the amplified pressure must be sustained over the distance approximately equal to the single shock time to detonation distance corresponding to the amplified pressure,² and (3) the pressure must be sustained over a width of explosive approximately the same as the failure radius of the explosive.³ These conditions are the same used for any shock to estimate whether initiation might occur, the only difference is that we are applying them to a local shock structure that occurs from a boundary interaction.

All the experimental work reported here involves the initiation of PBX 9502 by reflected waves from titanium boundaries. For PBX 9502, we found that irregular reflection was most likely to result in initiation. The primary reason is that the irregular reflection results in an amplified pressure wave running into explosive that was not preshocked. This wave structure, often referred to as a Mach stem or Mach reflection, is not the classical triple-point solution, but rather a curved stem structure. We will discuss the analysis that suggests shock initiation with an irregular reflection or Mach reflection is possible, two experiments in which such initiation was detected for PBX 9502, and possible situations that may deplete or enhance the effect.

CHARACTERIZATION OF REFLECTIVE WAVE BEHAVIOR

FOCAL ANALYSIS

The geometrical configuration we studied is a plane shock incident on a flat titanium plate. We applied the

classical shock polar theory), shown in Fig. 1, to shock reflection in explosive, with appropriate equations of state (see Table I).

When a shock wave obliquely encounters a high impedance interface, two basic kinds of shock reflection occur. Regular reflection is the case in which the incident wave and the reflected wave intersect at the interface (Fig. 1a). Irregular reflection includes all other possibilities, of which there are many. The most famous is regular reflection by "classical" Mach reflection in which

the interaction results in a triple-shock structure and a contact discontinuity separating the double-shocked material from the single-shocked material that has flowed through the step structure (see Fig. 1c). For brevity, any wave reflection structure that features a step, where a single shock processes material from zero pressure to the amplified pressure behind the reflection, will be called a Mach reflection.



FIGURE 1. REGULAR AND MACH REFLECTION FLOW DIAGRAMS

TABLE I. SUB-GRIESEN EQUATION OF STATE PARAMETERS

Material	Density kg/m^3	Shock Hugoniot GPa-m/s	Griesssen Gama
PPX 1801 ^a	1.894	0.236 x 1.796	1.3
Bleumont	18.94	0.251 x 1.516	1.3

In the local shock polar analysis, the flow in the regions delineated by the shocks is assumed to be one-dimensional. Shock jump conditions (conservation of mass, momentum, and energy subject to the equations of state) are satisfied across each shock. The incident shock turns the flow toward the wall and the reflected wave turns the flow back away from the wall. At the walls, the boundary conditions are such that the flow behind the shock structure must be parallel to the flow in the wall and pressure is continuous across the boundary. An irregular reflection appears when a regular reflection cannot meet this compatibility condition.

The shock polar in the pressure-flow angle plane is a convenient means of examining the possible solutions. Figure 2 indicates how the shock polar is generated: the phase velocity V_{ϕ} is fixed and the angle α between this velocity vector and the shock k is varied. Jump conditions are used to calculate the normal component of the velocity behind the shock, and because the tangential component is unaltered, the flow angle can also be found. Flow angle α and the pressure, the two variables of interest, are plotted in Fig. 2. The polar labeled I indicates the states achievable behind the incident shock. The polar labeled R indicates the states achievable behind the

reflected shock, arising from the state behind the incident shock. The polar labeled T indicates the states achievable behind the shock transmitted in the material. In regular reflection (see Fig. 1a), the flow behind the shock structure satisfies the boundary conditions at the intersection of the I and R polar, where the flow across the wall is parallel and no pressure gradient exists across the wall.



FIGURE 2. VELOCITY DECOMPOSITION OF THE FLOW ACROSS A SHOCK

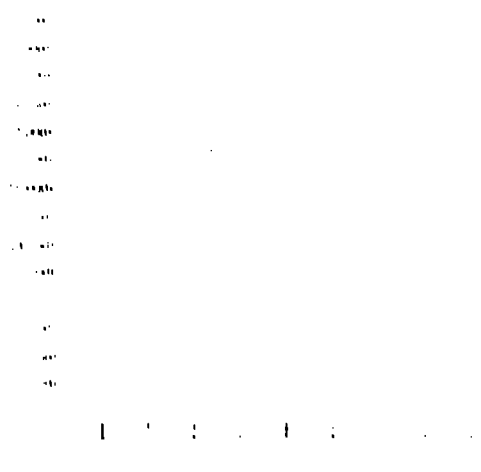


FIGURE 3a. SHOCK POLAR FOR REGULAR REFLECTION IN PBX 9501.

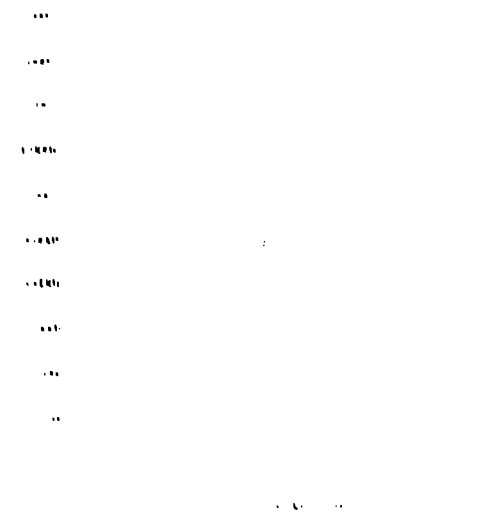


FIGURE 3b. SHOCK POLAR FOR IRREGULAR REFLECTION IN PBX 9501.

In Mach reflection (see Fig. 3b), the E and R polaras do not intersect. If E and R had intersected at more than one point, a "classical" Mach reflection would be a possible solution. In this case, however, the incident shock will curve as the wall is approached. If the flow is quasi steady, this analysis can be continued — this assumption is equivalent to assuming that the stem does not grow on a time scale of interest in these calculations. Continuing, we find that the flow behind the Mach stem at the wall is specified by the intersection of the E and I polaras. Furthermore, the state on the curved Mach stem it precisely displaced from the wall by on the E polar between the intersection of E with the E and R polaras. Because of this continuous variation, the precise

definition of the size of the Mach stem or its growth rate is lost. However, the shape of the E polar indicates that some regime of the flow will have reached amplified pressure levels through a strong shock (the top of the shock front is relatively flat). Later, the wall pressure in this solution will be used as the stem pressure estimate.

Solutions to the reflection problem can also be plotted in the pressure-deflection angle plane. In this case, the wall pressure behind the reflected wave is given as a function of the interaction angle for fixed incident shock pressure. That was done for a 4.2 kbar incident shock in Fig. 4.

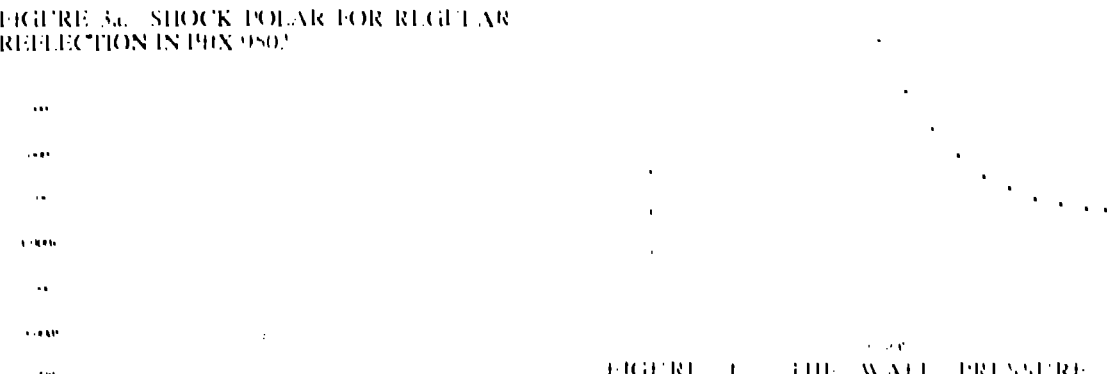


FIGURE 4. THE WALL PRESSURE-INTERACTION ANGLE PLOT FOR A 4.2 kbar SHOCK. THE OPEN POINTS INDICATE REGULAR REFLECTION, WHILE AS THE SOLID POINTS INDICATE IRREGULAR MACH REFLECTION.

In either normal or Mach reflection, the pressure is elevated to a level that will initiate unclocked PBX 9501. In regular reflection, the elevated pressure propagates into material that has been preshocked and densitized by the incident wave to some extent. In Mach reflection, however, the stem, with sufficiently elevated pressure behind it, propagates into unshocked explosive and represents a likely initiation mechanism. The shock polar analysis is convenient for giving visual insight and estimates of pressures; however, the analysis does not lead to any growth rate information, nor does it examine the stability of the flow configuration. To answer these questions, we examined the flow with the MESA hydrodynamic code.

HYDROCODE ANALYSIS

With MESA, we calculated several reflected-wave solution pressures and interaction angles (using a 128-mesh) shown in Figs. 5–7. The definition of a

17. A high-gradient shock obliquely impacting a 1-mm thick aluminum plate at 30° incident angle. 22. as after the initial impact of the plate. Here a significant shock stem leads the incident shock. The 1.20 kbar region (dark) is a stagnation portion of the stem and the 1.80 kbar contour extends into the reflected wave region. Even if the shock wave looks rather straight in this region, there is curvature in the shock wave and a more obvious continuous rise in shock pressure as the wall is approached.

Although these calculations are rather straight forward to compute and analyze, a subtle detail exists at the beginning of the calculation as how to resolve the initial

singularity on a finite grid. In these calculations we took no special precautions, and if one looks carefully at the stem width in time, it appears to grow more rapidly at early times, then slows its growth slightly later, and finally reaches an intermediate value. This appears to be the result of not being able to resolve the singularity at the beginning of the calculation. Hence, at early times in the calculation, the calculation appears to overestimate the stem width and underestimate the pressure. This problem appears to resolve itself in time; however, some caution should be used in the examination of early results from the simulation.

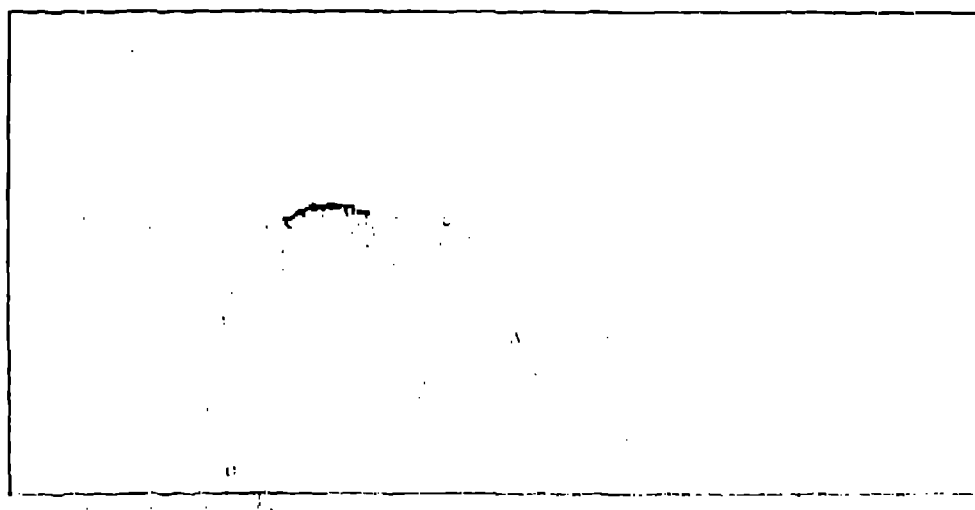


FIGURE 5. MESA CALCULATION OF A 1.2 kbar SHOCK INCIDENT ON A 1-mm THICK ALUMINUM PLATE. PRESSURE CONTOURS ARE FABRICATED IN KILOCARAS.

In summary, the hydrocode simulations are in qualitative agreement with the shock polar analysis, although the pressure values from the hydrocode tend to have somewhat lower pressures than the estimates from shock polar theory. The growth angle of the stem region found in these calculations ranges from 1 to 5°, depending on the incident shock pressure and angle. The small growth angles can be used to rationalize the use of the quasi-steady approximation in the previous section. This range of angles is typical for growth rates of Mach stems seen in gas dynamics⁵ and detonation experiments.⁶

INITIATION ANALYSIS

The procedure analysis has shown that in either end-on or oblique reflection, the pressure amplituon is sufficiently large to dramatically reduce the distance for detonation of unshocked explosive.⁷ To examine the possibility of detonation by a circular reflection, many cases can be ruled out because the flow behind the second shock is freely supersonic and any energy release

in the double-shocked material has no possibility of influencing either the reflected or the incident shock. As the incidence angle approaches the critical angle, the incident cannot be used before the flow behind the reflected shock becomes subsonic. In the analysis consider the thickness of material that can travel through the incident shock and reach the second shock before it has been densitized by the incident shock. This width can be estimated by assuming the time that the material is in the incident shock region must be less than the time it takes for the explosive to be densitized. We used the time estimate from Campbell and Travers' paper⁸ for PBX 9501, because no densitization data are available for PBX 9501. For a 1.2 kbar shock at 30° incidence angle, the width of material at the second shock remains constant to the criterion of 1 mm, which is much smaller than the self-sustained detonation thickness, and even smaller than the sum of detonation distance for the explosive to the double-shocked explosive region. This condition may exist, but it has low probability of developing into a detonation because it is significantly smaller than the detonation radius.⁹ A more definitive conclusion is predicted by using the self-sustained radius criterion for

precompressed explosive has never been studied. This initiation scenario may be much more important in more sensitive explosives like PBX 9501. These have much smaller tailgate thicknesses than do insensitive explosives, and much lower incident shock pressures result in much larger critical angles. In all, we were led to examine the Mach reflection regime, where prestack was not an issue.

In Mach reflection, with sufficiently elevated pressure behind it, the stem propagates into undrilled explosive and presents a likely initiation case because the explosive has not been desensitized. Another aspect of Mach reflection enhances the likelihood of a situation in which initiation can occur: the flow behind a large portion of the curved shock wave section is antisonic. This implies that energy release from the shocked explosive has a chance of reinforcing the shock wave and of building to a detonation wave.

The remaining requirement is that the Mach stem must be sufficiently large. Classical shock polar analysis provides no steady growth information in this curved stem case. However, the hydrocode calculations indicated a growth angle of 4–6°. This would imply that initiation would occur after a run of 1.1 to 1.9 mm along the surface of the uranium plate, depending on the shock pressure and angle. Using this analysis, we designed the experiments to detect the transition from shock to detonation when a 40-kbar plane shock in PBX 9501 is reflected from a flat uranium plate with an incidence angle of 40° and 50°.

EXPERIMENTAL RESULTS

The PBX 9501 test pieces were six-sided prisms (see Fig. 6). Top and bottom surfaces defined two horizontal planes 0.64 cm apart. Two sideset detuned planes that were perpendicular to the top and bottom planes. One of the other two surfaces (A in Fig. 6) was angled at 30° in the bottom plane and was defined as the observation surface. The other surface (B in Fig. 6) was angled at 40° or 50° with respect to the bottom plane and was covered with a 3-mm-thick uranium plate providing the reflective boundary. A plane shock wave was driven into the bottom of the prism with the plane-wave attenuator system shown in Fig.

The phase velocity of the wave along the uranium surface, the width of the Mach stem, and the incident wave velocity, pressure, and position must be observed to obtain a complete experimental record of the experiment. The shock arrival time along the uranium surface (II) was monitored with a series of time-of-arrival pins that we placed at known distances along the uranium plane. Each pin reported the time at which the shock transmitted tailgate angle through the uranium plate arrived at the free surface. We evaluated the phase velocity of the wave at the explosive-metal interface from these data by assuming the flow to be steady. We obtained the width, shape, and velocity of the Mach stem as well as the incident wave velocity by using a multiple-stuttering camera technique. The intersection of surfaces A and II had at least 25 mm of surface A were observed with a series of arced thermocouples. The camera was altered

and a record of the fast-gate tie-wave arrival time of the Mach stem and incident shock at 11 different cut distances into the explosive.

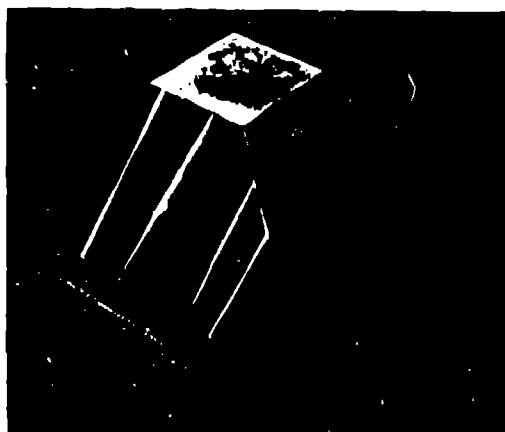


FIGURE 6. PBX 9501 TEST PIECE WITH CRANIUM PLATES ATTACHED

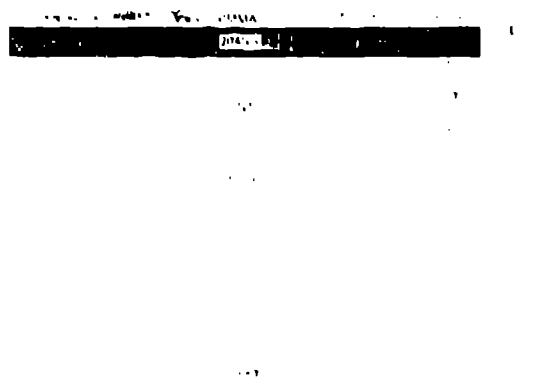


FIGURE 7. THE PLANE-SHOCK DRIVER SYSTEM USED TO DRIVE A 40-kbar SHOCK INTO THE TEST PIECE (9.0-cm dimensions are in mm). L.E.P.

down in Fig. 8 are the shock arrival times on the uranium surface for the 40° experiment. Straight lines show that the incident phase velocity associated with the propagation of the first Mach reflection is about 10.2 km/sec. About 75 mm from the corner, a transition to 7.4 km/sec occurs. Similar results for the 50° interaction angle, also shown in Fig. 8, indicate that the wave accelerates from 9.2 km/sec to 7.68 km/sec after transiting the surface for 30 mm.

In Fig. 9 is the digitized camera record from the 40° shot, and the smear-camera record of the 50° experiment is shown in Fig. 10. Each shot was obtained so that a record of the wave arrival time was obtained for a constant distance from the bottom surface of the prism. Figure 9 recorded the arrival of the incident wave at a

horizontal line in the region away from the aluminum interface. These were used to obtain the velocity of the incident shock and thus to estimate the incident pressure. The Mach stem developed at the uranium/PBX 9502 interface was recorded as the early arrival part of each trace. When the location of the break in the horizontal trace was measured, the width of the Mach stem or detonation front could be estimated as a function of run distance along the uranium plate. Assuming that the Mach stem is normal to the wall, a conservative estimate for the Mach stem width can be obtained. The assumption that the Mach stem is normal to the wall may be relaxed if one is willing to accept a calculated value for this angle. Mach stem width data are plotted as a function of position along the uranium plate in Fig. 14. A sudden change in wave width is associated with the transition to detonation. This is in good agreement with the previously described pin data. The last shot recorded a detonation wave 7 mm wide in the 40° case and 17 mm wide in the 50° case.

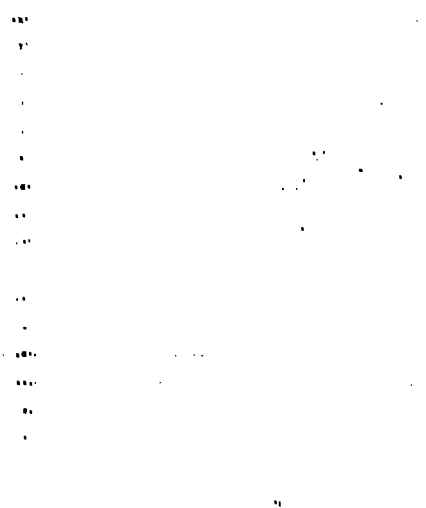


FIGURE 8. PIN DATA FOR SHOT No. C-649c AND C-6513.

The two nuclear cameras records clearly show the development of curved Mach stems with growth angles of 17° and 36°. The transition occurred when the stem reached a width between 3 and 4 mm in the 40° case and between 4 and 6 mm in the 50° case. After the transition, a detonation wave is clearly observed with a growth angle of more than 3° in the 40° incident angle case and more than 15° in the 50° case. We expect that this angle is strongly influenced by corner turning and preshock desensitization processes. These times to detonation, measured from the driver system are 1.5 of what one would expect from extrapolating existing cone to detonation data to the incident shock pressure.



FIGURE 9. DIGITIZED SMEAR CAMERA RECORD FOR SHOT No. C-649c. INCIDENT SHOCK WAS 3.5 kbar AT 30° INCIDENT.

DISCUSSION

These experiments demonstrate that, in PBX 9502, a Mach reflection can transit into a detonation for two different incident angles. Diameter effect data³ indicate that a 7 mm radius rate stick of PBX 9502 would detonate at 7.19 kbars and a 17 mm radius rate stick detonates at 7.16 kbars. The final ion velocities agree well with these values. Minimum width of the detonation observed is about 4 mm, and this is close to the radius of 4.5 mm for PBX 9502.⁴ Pressure behind the Mach stem was estimated at 169 kbar for 40° and 100 kbar at 50° based on the shock polar theory. Required detonation distance for a planar, wet-supported shock at these pressures is about 3 mm and 13 mm, respectively.⁵ Our experiments saturated the shock pressures much lower than this. However, the flow behind the stem shock is substantially more complicated than that found in a wedge experiment. Therefore, the conditions we detected are in agreement with our expectations derived from other aspects of explosive behavior. Because the shock initiation estimates of where detonation occurs appear to hold, one would expect a multiple-shock-front model to be able to model these problems adequately. Calculations⁶ done by Ed Koder show that this is indeed true and give extra evidence that the transitions in these cases are due to the shock reflection process.

Further work continues on this topic in the areas of other explosive materials, divergence effects of the incident shock wave, and the effect of convergent and divergent wall interfaces. We are using PBX 9501 to assess the implications of the initiation mechanism for much more sensitive explosives. The calculations indicates that for PBX 9501, the angles at which Mach stems become important are about 30°, greater than those of PBX 9502, probably because the pre-ignition of the detonation

from a flame shock occurs are significantly smaller. Although the range of possible angles is smaller, the initiation appears likely because the failure diameter is much smaller and the run to detonation is significantly shorter than for that of PBX 9502. Also, for PBX 9501, some cases of initiation by regular reflection may be possible.

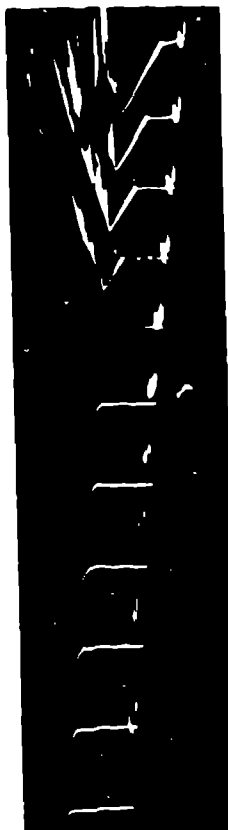


FIGURE 10. SMEAR CAMERA RECORD FOR SHOT No. C-6584. INCIDENT SHOCK WAS 1.2 kbar AT 50° INCIDENCE. FOR EACH SET, TIME IS INCREASING IN THE VERTICAL DIRECTION. THE OVEREXPOSURE ON THE STEM IN THE LAST FOUR SETS IS DUE TO THE BRIGHT FLASH RESULTING FROM THE DETONATION, AS COMPARED WITH THE EXPOSURE OF THE INCIDENT SHOCK.

Divergence can occur in two different ways; the incident shock can diverge or the metal boundary can curve away from the incident shock. In both of these cases, computer simulations show that the formation of the Mach stem is inhibited. Experiments are currently being designed to examine these effects. We have only begun to study convergent geometries that we expect will enhance the formation of Mach stems.

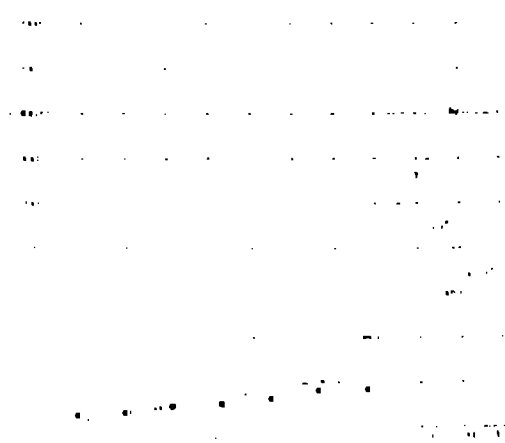


FIGURE 11. STEM WIDTH MEASUREMENTS FOR SHOT Nos. C-6496 AND C-6513. THE SOLID SQUARES ARE STEM WIDTHS MEASURED FROM THE MI-SA CALCULATION OF THE REFLECTION OF A 1.2 kbar SHOCK INCIDENT AT 30° ON A FRANQUIM SURFACE.

In summary, we have experimentally observed the transition of a Mach reflection into a detonation in PBX 9502. This initiation mechanism can radically reduce the run to detonation in explosive charges with high impedance boundaries. Classical analysis can bound the incident shock curvature and angles of Mach reflection initiation. The resulting shock configurations and knowledge of explosive behavior can be used to help decide whether initiation is likely. However, growth angle and stem size information is not found by means of the classical analysis. Computer simulations are useful for obtaining growth angle estimates, and Lorentz-Eire models can be used to examine the initiation process. Even so, there are still mesh resolution problems to address, and equation of state or specially sensitive material information for the explosive at low pressures will need to be refined before simulations are reliable. Therefore, further experiments and analysis will be necessary to completely describe the initiation criterion for shock reflection from high impedance boundaries.

ACKNOWLEDGMENTS

We express our appreciation to Victor Sandoval, Willie Spencer, Rudy Atchuleta, Bob Crutchfield, Andreas Krause, and Walter Quintana, who were responsible for, or assisted in, fitting these experiments. We thank Ed Kobler for discussions while using Lorentz-Eire simulations of initiation by shock wave reflection. We acknowledge that LeRoy Green had the insight to suggest the possibility of initiation by a Mach stem. We thank John Rattner for many helpful discussions and support. We also thank Gary Hauck and John Rattner for their persistent support in obtaining funding.